Improved hydrogen desorption properties of Co-doped Li$_2$BNH$_6$

ZHENG XueLi[1,2], WU GuoTao[2*], HE Teng[2], CHU HaiLiang[2], CHEN Hua[1] & CHEN Ping[2]

[1] *Key Lab of Green Chemistry and Technology, Ministry of Education, the Institute of Homogeneous Catalysis, College of Chemistry, Sichuan University, Chengdu 610064, China;*
[2] *Dalian Institute of Chemical Physics, Chinese Academy of Sciences, Dalian 116023, China*

The hydrogen desorption properties of Li$_2$BNH$_6$ were improved by doping with cobalt. With the addition of CoCl$_2$ (7 wt%), more than 8 wt% of hydrogen was released from Li$_2$BNH$_6$ at temperatures below 210°C, which is approximately 90°C lower than that of pristine Li$_2$BNH$_6$. X-ray diffraction, Fourier transform-infrared and Raman characterizations revealed that the dehydrogenation was a stepwise process with the formation of intermediates Li$_4$BN$_3$H$_{10}$ and LiBH$_4$ and final products of Li$_3$BN$_2$ and LiH. The introduction of Co greatly accelerated the dehydrogenation of Li$_4$BN$_3$H$_{10}$. X-ray absorption near-edge structure measurements revealed that Co and CoB species formed during ball milling of CoCl$_2$ with LiBH$_4$ and LiNH$_2$, which may function as catalyst in the subsequent dehydrogenation.

lithium amide, cobalt, lithium borohydride, hydrogen release

To meet the requirements for hydrogen fuel cell technology, tremendous efforts have been devoted to the development of hydrogen storage materials with high hydrogen contents [1]. Alanates [2], borohydrides [3], amide-hydride systems [4–7], ammonia borane [8,9], and metal amidoboranes [10,11] have been explored as potential hydrogen storage materials. LiBH$_4$ with a hydrogen capacity of 18.4 wt% [12], has attracted considerable research attention [3]. However, its thermal decomposition to LiH + B + 3/2H$_2$ is a highly endothermic process (approximately 67 kJ mol^{-1} H$_2$) [13], and has a relatively high kinetic barrier [3], and thus requires high temperatures (320–600°C) [3]. Several attempts to improve the thermodynamic properties of hydrogen release from LiBH$_4$ have been made by reacting LiBH$_4$ with chemicals such as SiO$_2$ [3], MgH$_2$ [13] and CaH$_2$ [14]. Recent investigations revealed that complex hydrides (LiAlH$_4$, LiBH$_4$ and NaAlH$_4$) could be destabilized by reaction with alkali and alkali earth amides. It was reported that approximately 8.1 wt% of H$_2$ can be released from 2LiAlH$_4$-LiNH$_2$

at 85–320°C [15]. Four equivalent of H$_2$ were also found to evolve from 1LiAlH$_4$-2LiNH$_2$ at 50–500°C [16]. Similar improvements were achieved by mixing LiBH$_4$ with amides. Ball milling LiBH$_4$ with 2 equivalent of LiNH$_2$ produces Li$_3$BN$_2$H$_8$, which can release >10 wt% of H$_2$ at 250–350°C [6,7]. In these hydride-amide systems where protic H and hydridic H coexist, the large potential for the combination of oppositely charged H atoms to form H$_2$ and the establishment of a strong B–N (or Al–N) bond should be the driving force for the favorable dehydrogenation. A series of quaternary complex hydrides, such as Li$_2$BNH$_6$, Li$_3$BN$_2$H$_8$ and Li$_4$BN$_3$H$_{10}$, can be prepared by mechanically milling LiBH$_4$ and LiNH$_2$ with various molar ratios [17]. However, those complex hydrides encounter very large kinetic barriers in dehydrogenation [6,18]. The LiBH$_4$-LiNH$_2$ system can be catalytically modified with transition metal additives, such as PdCl$_2$, Pt/Vulcan carbon, NiCl$_2$, CoCl$_2$, can greatly reduce the dehydrogenation temperature [19–21]. In particular, >9 wt% of H$_2$ can be released from Li$_3$BN$_2$H$_8$ at ca. 182°C in the presence of 5 wt% of Co-based catalyst [20]. Approximately 7.5 wt% of H$_2$ was released from

*Corresponding author (email: wgt@dicp.ac.cn)

$Li_4BN_3H_{10}$ at 160–260°C with the addition of 11 wt% of $NiCl_2$ [21]. Co-based additives were also found to have a catalytic effect on the hydrogen release from boron-containing hydrogen storage materials [22,23]. The hydrogen capacity of Li_2BNH_6 ($1LiBH_4$-$1LiNH_2$) is 13.3 wt%, which is higher than that in $Li_3BN_2H_8$ (11.8 wt%) or $Li_4BN_3H_{10}$ (11.0 wt%). However, there are few reports on the catalytic modification of this complex hydride. Herein, the dehydrogenations of pristine and the Co-doped Li_2BNH_6 are systematically investigated. It was found that the Co-additive promoted the dehydrogenation kinetics of Li_2BNH_6. The pathway of dehydrogenation was identified by X-ray diffraction (XRD), and Fourier transform-infrared (FT-IR) and Raman spectroscopy characterizations.

1   Materials and methods

$LiBH_4$ (95%), $LiNH_2$ (95%) and anhydrous $CoCl_2$ (97%) were purchased from Acros, Fluka and Sigma-Aldrich, respectively. To prevent oxygen and moisture contamination, all the sample loading and handling operations were conducted in an MBRAUN glovebox filled with purified argon. A mixture of $LiBH_4$-$LiNH_2$ (molar ratio 1:1) was mechanically milled with 7 wt% of $CoCl_2$ using a planetary Retch PM 400 mill. The ball-to-sample mass ratio was about 30:1. The rotation speed was regulated at 200 r/min and the milling time was 8 h. At the end of ball milling the vessels were connected to a pressure gauge to measure the pressure inside. Then, the gaseous products were passed through a mass spectrometer (MS) for analysis. In contrast to the undoped $LiBH_4$-$LiNH_2$ sample, a small amount of H_2 (0.07 equivalent) was generated during ball milling.

A temperature-programmed desorption (TPD) system connected with a MS was constructed in our laboratory and used to investigate gas release. Approximately 50 mg of sample was loaded and tested each time. The temperature was increased to 500°C at 2°C/min. The carrier gas was purified argon and the flow rate was set at 40 mL/min. Quantitative measurements on hydrogen release were performed on a commercial automatic Sieverts-type apparatus (Advanced Materials Co.). A sample of approximately 150 mg was tested with a heating rate of 2°C/min. The ammonia concentration in the gaseous product was measured by a Thermo conductivity meter with an accuracy of 0.1 μs/cm. The NH_3 concentration was proportional to the decrease in the ion conductivity measured after the outlet gas was passed through a dilute H_2SO_4 solution. A PANalytical X'pert diffractometer equipped with Cu Kα radiation (40 kV, 40 mA) and an *in situ* cell was employed for structural identification. FT-IR measurements were conducted on a Varian 3100 FT-IR spectrometer. Raman spectra were recorded on a commercial micro-Raman spectrometer (Renishaw, UK) using a He/Ne laser with a wavelength of $\lambda =$

514 nm. X-ray absorption near-edge structure (XANES) spectra were collected in fluorescence mode at the X-ray absorption fine structure (XAFS) station of the Shanghai Synchrotron Radiation Facility (SSRF, Shanghai). Samples for XAFS measurements were pressed into pellets in glovebox to avoid air contamination. Metallic cobalt foil and cobalt chloride were also measured as references and for energy calibration.

2   Results and discussion

2.1   Hydrogen desorption from Li_2BNH_6

Li_2BNH_6 can be prepared by mechanically milling $LiBH_4$ and $LiNH_2$ in a molar ratio of 1:1 [17]. In this study, formation of Li_2BNH_6 was observed by XRD in the pristine and Co-doped samples after 8 h of ball milling. The results of TPD measurements on the pristine and Co-doped Li_2BNH_6 samples are shown in Figure 1. For the pristine sample, hydrogen desorption began at approximately 170°C and peaked at 295°C. The second step of desorption started at 370°C and reached the maximum desorption rate at around 410°C. This dehydrogenation behavior is different from that of $Li_3BN_2H_8$ and $Li_4BN_3H_{10}$ [6,7,21]. By contrast, the Co-doped sample began to release hydrogen at approximately 110°C, and reached the maximum desorption rate at approximately 230°C, which is about 65°C lower than that of the pristine Li_2BNH_6. However, little improvement was observed in the second step of dehydrogenation. Quantitative measurements of hydrogen desorption from the pristine and Co-doped samples were conducted on a Sieverts-type apparatus. As shown in Figure 2, approximately 3.9 equivalent of H (8.6 wt%) was evolved from the pristine Li_2BNH_6 sample at 170–300°C. In total, 5.3 equivalent of H (11.7 wt%) was desorbed when the temperature approached 450°C. An acceleration of hydrogen release at about 290°C was observed, which was consistent with the TPD result. Nevertheless, it is clear that a large kinetic
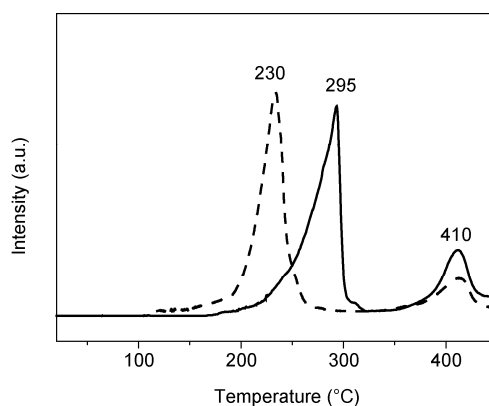
Figure 1   TPD-MS H_2 spectra of pristine (solid line) and Co-doped Li_2BNH_6 samples (dotted line).
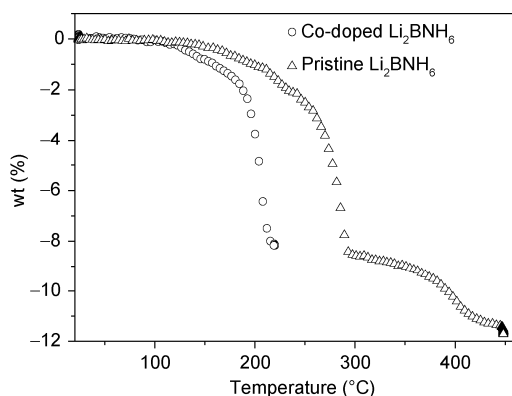
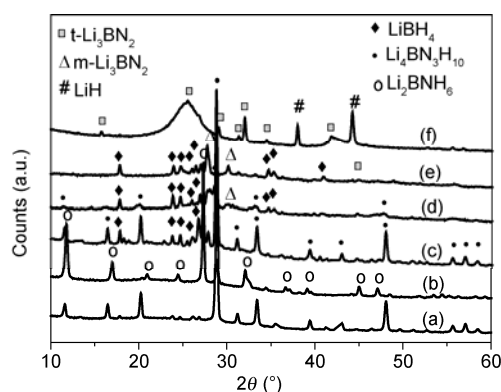**Figure 2** Volumetric release of hydrogen from pristine and Co-doped Li_2BNH_6 samples.

Figure 4 FTIR spectra of (a) $Li_4BN_3H_{10}$, (b) Co-doped Li_2BNH_6 after ball milling, and the samples collected after (c) heating at 90°C, and release of (d) 2.2, (e) 3.9 and (f) 5.3 equivalent of H.
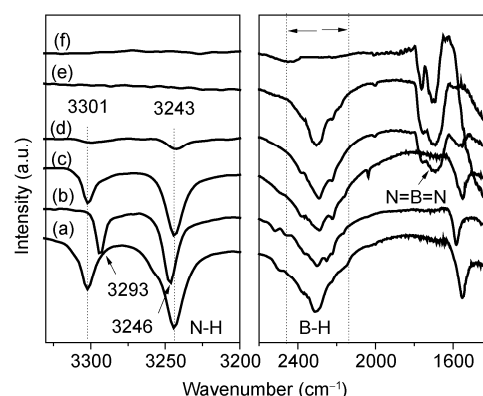
barrier resulted in hydrogen evolution occurring at higher temperatures. Introduction of $CoCl_2$ into Li_2BNH_6 resulted in hydrogen evolution at approximately 110°C and acceleration of dehydrogenation was observed at around 200°C. This is a major improvement compared with the pristine Li_2BNH_6. Approximately 3.9 equivalent of H (8.1 wt%) was desorbed in the first step at <210°C. The concentration of NH_3 in the gaseous phase was below 890 ppm.

2.2 Dehydrogenation mechanism

As shown in Figure 1, dehydrogenation of Li_2BNH_6 is a two-step process. In order to gain insight into the reaction path, the Co-doped samples collected after ball milling and dehydrogenation at different stages were analyzed by XRD, FTIR, and Raman analyses. After 8 h of ball milling, the $LiBH_4$, $LiNH_2$ and $CoCl_2$ reagents had disappeared and a new set of diffraction peaks attributed to Li_2BNH_6 was observed (Figure 3(b)) [17]. In the FTIR spectrum (Figure 4(b)) obtained after ball milling, peaks at 3293 and 3246 cm^{-1} were assigned to the symmetric and asymmetric N–H stretching vibrations of Li_2BNH_6 [24]. The corresponding
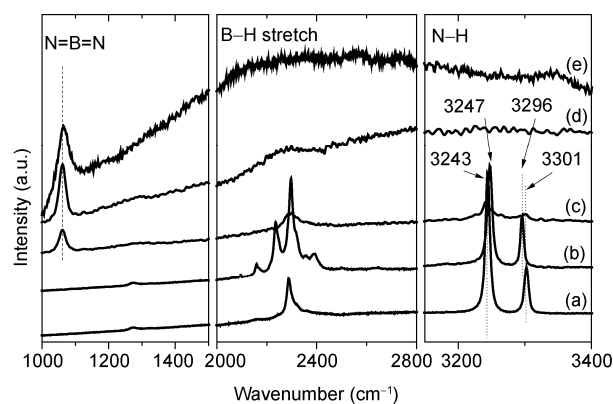
Raman spectrum of Li_2BNH_6 (Figure 5(b)) also displayed peaks for the N–H vibrations at 3296 cm^{-1} and 3247 cm^{-1}, and the B–H vibrations at 2159 cm^{-1} (w), 2236 cm^{-1} (sh), 2296 cm^{-1} (s), and 2390 cm^{-1} (w). Upon heating the Co-doped Li_2BNH_6 sample at 90°C, $Li_4BN_3H_{10}$ and $LiBH_4$ rather than Li_2BNH_6 were observed as the dominant phases by XRD (Figure 3(c)). FTIR spectrometry revealed that the peaks for the N–H vibrations had shifted to 3301 cm^{-1} and 3243 cm^{-1} (Figure 4(c)). The intensities of the N–H stretches decreased after approximately 2.2 equivalent of H was desorbed and a broad band centered at about 1680 cm^{-1} developed, which can be assigned to the vibration of N=B=N in Li_3BN_2 [25]. After releasing about 3.9 equivalent of H atoms at <210°C, the N–H stretches disappeared and the broad band at 1680 cm^{-1} intensified.
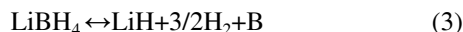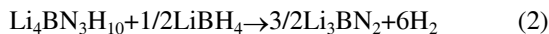
After release of about 5.3 equiv. of H the B–H stretches disappeared (Figure 4(f)). XRD characterization (Figure 3) indicated that the $Li_4BN_3H_{10}$ phase was gradually weakened during dehydrogenation, and this was accompanied by a gradual increase of the monoclinic phase of Li_3BN_2 [26]. Finally, after the evolution of 5.3 equivalent of H at

Figure 3 XRD patterns of (a) $Li_4BN_3H_{10}$, (b) Co-doped Li_2BNH_6 after ball milling, and the samples collected after (c) heating at 90°C, and release of (d) 2.2, (e) 3.9 and (f) 5.3 equivalent of H. t-Li_3BN_2 and m-Li_3BN_2 reflect the tetragonal and monoclinic phases of Li_3BN_2, respectively.

Figure 5 Raman spectra of (a) $Li_4BN_3H_{10}$, (b) Co-doped Li_2BNH_6 after ball milling, and the samples collected after release of (c) 2.2, (d) 3.9 and (e) 5.3 equivalent of H.

<450°C, LiBH$_4$ disappeared and LiH and tetragonal Li$_3$BN$_2$ appeared. In accordance with the XRD and FTIR characterizations, Raman spectra show the gradual decrease of the N–H and B–H vibrations, and the development of the N=B=N vibration in Li$_3$BN$_2$ (1060 cm^{-1}) (Figure 5) [27].

The pristine Li$_2$BNH$_6$ samples at different stages of dehydrogenation were also collected for structural characterization. The results showed an almost identical process with that of the Co-doped sample although the dehydrogenation occurred at much higher temperatures. This indicates that the main reaction pathway is unchanged by the introduction of CoCl$_2$. Upon heating to approximately 90°C, the conversion of Li$_2$BNH$_6$ to Li$_4$BN$_3$H$_{10}$ and LiBH$_4$ takes place (reaction (1) [28]. Hence, the decomposition of Li$_2$BNH$_6$ is likely to occur through dehydrogenation of Li$_4$BN$_3$H$_{10}$ + 1/2LiBH$_4$ (reaction (2)) and then that of LiBH$_4$ (reaction (3)). Therefore, the hydrogen release from the Co-doped and pristine Li$_2$BNH$_6$ can be expressed as follows:

$$Li_2BNH_6 \rightarrow 1/3Li_4BN_3H_{10} + 2/3LiBH_4 \qquad (1)$$

$$Li_4BN_3H_{10} + 1/2LiBH_4 \rightarrow 3/2Li_3BN_2 + 6H_2 \qquad (2)$$

$$LiBH_4 \leftrightarrow LiH + 3/2H_2 + B \qquad (3)$$

Li$_4$BN$_3$H$_{10}$ releases hydrogen exothermically and its rehydrogenation is thermodynamically unfavorable [29]. Storage and release of hydrogen by LiBH$_4$ is partially reversible [30]; therefore, the Li$_2$BNH$_6$ storage system may be partially reversible.

2.3 Chemical state of Co catalyst

After ball milling LiBH$_4$ and LiNH$_2$ with 7 wt% of CoCl$_2$ for 8 h, 0.07 equiv alent of H$_2$ was generated and the sample changed color from white to black. This indicates that the reduction of CoCl$_2$ occurred during the milling process. However, no Co-related phases were observed in the XRD pattern, which is probably due to the low loading and/or poor crystallinity. More information regarding the chemical state and local environment of Co were obtained from the XAFS analyses. The XANES of the freshly ball-milled sample resembled that of metallic Co (Figure 6), which indicates that reduction of CoCl$_2$ by LiBH$_4$ occurred during ball-milling. Fourier transformation of the XAFS spectra showed that the ball milled sample had a dominant peak at around 2.53 Å with a shoulder at 1.94 Å (Figure 7), which are close to the second shell Co-Co distance (2.67 Å) and the first shell Co-B distance (2.08 Å) of CoB, respectively [31]. As Tang et al. [20] revealed, both Co and CoB species have catalytic effects on the dehydrogenation of Li$_3$BN$_2$H$_8$. Similarly, in the present case, Co and CoB species might also co-function as the catalyst. Co particles might have poor crystallinity and are finely dispersed in the sample, which leads to a high catalytic efficiency. It is likely that the Co particles could facilitate the formation of Li$_3$BN$_2$, and consequently decrease the dehydrogenation temperature and
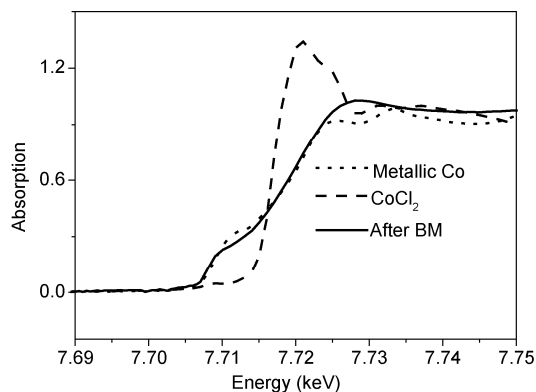
Figure 6   Co K-edge XAFS spectra of metallic Co, CoCl$_2$ and post-milled Co-doped Li$_2$BNH$_6$.
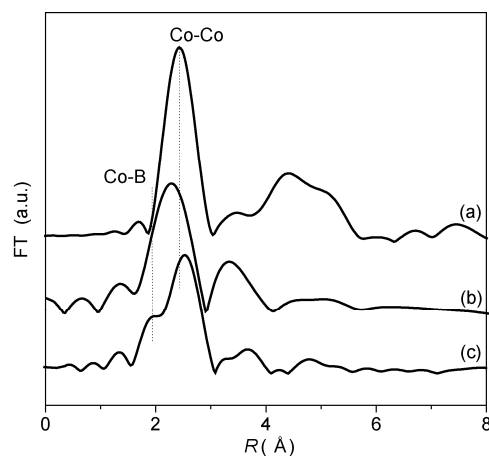
Figure 7   Fourier transformed spectra of (a) metallic Co, (b) CoCl$_2$ and (c) post-milled Co-doped Li$_2$BNH$_6$.

improve the dehydrogenation kinetics, as well as in the Co-doped dehydrogenation of NH$_3$BH$_3$ and Li$_3$BN$_2$H$_8$ [32,33].

3 Conclusion

Li$_2$BNH$_6$ undergoes a stepwise dehydrogenation with initial transformation into Li$_4$BN$_3$H$_{10}$ and LiBH$_4$ at about 90°C. Subsequent decomposition to Li$_3$BN$_2$ and H$_2$ occurs at around 300°C, and final full dehydrogenation to LiH, B and Li$_3$BN$_2$ occurs at 450°C. The addition of CoCl$_2$ (7 wt%) to Li$_2$BNH$_6$ greatly reduced the hydrogen desorption temperature. More than 8 wt% of hydrogen can be released at <210°C. XANES measurements revealed that Co and CoB were formed after ball milling of CoCl$_2$ with LiNH$_2$ and LiBH$_4$.

1 Schlapbach L, Züttel A. Hydrogen-storage materials for mobile applications. Nature, 2001, 414: 353–358

2 Bogdanović B, Schwickardi M. Ti-doped alkali metal aluminium hydrides as potential novel reversible hydrogen storage materials. J Alloys Compd, 1997, 253: 1–9

3 Züttel A, Wenger P, Rentsch S, et al. LiBH$_4$—A new hydrogen storage material. J Power Sources, 2003, 118: 1–7

4 Chen P, Xiong Z T, Luo J Z, et al. Interaction of hydrogen with metal nitrides and imides. Nature, 2002, 420: 302–304

5 Leng H Y, Ichikawa T, Hino S, et al. New metal-N-H system composed of Mg(NH$_2$)$_2$ and LiH for hydrogen storage. J Phys Chem B, 2004, 108: 8763–8765

6 Pinkerton F E, Meisner G P, Meyer M S, et al. Hydrogen desorption exceeding ten weight percent from the new quaternary hydride Li$_3$BN$_2$H$_8$. J Phys Chem B, 2005, 109: 6–8

7 Aoki M, Miwa K, Noritake T, et al. Destabilization of LiBH$_4$ by mixing with LiNH$_2$. Appl Phys A: Mater Sci Proc, 2005, 80: 1409–1412

8 Wolf G, Baumann J, Baitalow F, et al. Calorimetric process monitoring of thermal decomposition of B-N-H compounds. Thermochim Acta, 2000, 343: 19–25

9 Gutowska A, Li L Y, Shin Y S, et al. Nanoscaffold mediates hydrogen release and the reactivity of ammonia borane. Angew Chem Int Ed, 2005, 44: 3578–3582

10 Xiong Z T, Yong C K, Wu G T, et al. High-capacity hydrogen storage in lithium and sodium amidoboranes. Nat Mater, 2008, 7: 138–141

11 Diyabalanage H V K, Shrestha R P, Semelsberger T A, et al. Calcium amidotrihydroborate: A hydrogen storage material. Angew Chem Int Ed, 2007, 46: 8995–8997

12 Schlesinger H I, Brown H C. Metallo borohydrides. III. Lithium borohydride. J Am Chem Soc, 1940, 62: 3429–3435

13 Vajo J J, Skeith S L, Mertens F. Reversible storage of hydrogen in destabilized LiBH. J Phys Chem B, 2005, 109: 3719–3722

14 Yang J, Sudik A, Wolverton C. Destabilizing LiBH$_4$ with a metal (M = Mg, Al, Ti, V, Cr, or Sc) or metal hydride (MH$_2$, MgH$_2$, TiH$_2$, or CaH$_2$). J Phys Chem C, 2007, 111: 19134–19140

15 Lu J, Fang Z G Z. Dehydrogenation of a combined LiAlH$_4$/LiNH$_2$ system. J Phys Chem B, 2005, 109: 20830–20834

16 Xiong Z T, Wu G T, Hu J J, et al. Reversible hydrogen storage by a Li-Al-N-H complex. Adv Funct Mater, 2007, 17: 1137–1142

17 Meisner G P, Scullin M L, Balogh M P, et al. Hydrogen release from mixtures of lithium borohydride and lithium amide: A phase diagram study. J Phys Chem B, 2006, 110: 4186–4192

18 Noritake T, Aoki M, Towata S, et al. Crystal structure analysis of novel complex hydrides formed by the combination of LiBH$_4$ and LiNH$_2$. Appl Phys A: Mater Sci Proc, 2006, 83: 277–279

19 Pinkerton F E, Meyer M S, Meisner G P, et al. Improved hydrogen release from LiB$_{0.33}$N$_{0.67}$H$_{2.67}$ with metal additives: Ni, Fe, and Zn. J Alloys Compd, 2007, 433: 282–291

20 Tang W S, Wu G, Liu T, et al. Cobalt-catalyzed hydrogen desorption from the LiNH$_2$-LiBH$_4$ system. Dalton Trans, 2008: 2395–2399

21 Pinkerton F E, Meyer M S. Hydrogen desorption behavior of nickel-chloride-catalyzed stoichiometric Li$_4$BN$_3$H$_{10}$. J Phys Chem C, 2009, 113: 11172–11176

22 He T, Xiong Z T, Wu G T, et al. Nanosized Co- and Ni-catalyzed ammonia borane for hydrogen storage. Chem Mater, 2009, 21: 2315–2318

23 Chu H L, Xiong Z T, Wu G T, et al. Hydrogen storage properties of Ca(BH$_4$)$_2$-LiNH$_2$ system. Chem Asian J, 2010, 5: 1594–1599

24 Chater P A, David W I F, Johnson S R, et al. Synthesis and crystal structure of Li$_4$BH$_4$(NH$_2$)$_3$. Chem Commun, 2006: 2439–2441

25 Kulinich S A, Zhukov A N, Sevast'yanova L G, et al. On some alkali- and alkaline-earth-metal boron nitrides, unsaturated with boron. Diam Relat Mater, 1999, 8: 2152–2158

26 Yamane H, Kikkawa S, Horiuchi H, et al. Structure of a new polymorph of lithium boron nitride, Li$_3$BN$_2$. J Solid State Chem, 1986, 65: 6–12

27 Somer M, Herterich U, Curda J, et al. Ternary nitridoborates. 1. LiMg[BN$_2$] and Ba$_4$[BN$_2$]$_2$O, compounds with the anion [N-B-N]$^{3-}$: Syntheses, crystal structures, and vibrational spectra. Z Anorg Allg Chem, 1997, 623: 18–24

28 Chater P A, David W I F, Anderson P A. Synthesis and structure of the new complex hydride Li$_2$BH$_4$NH$_2$. Chem Commun, 2007: 4770–4772

29 Pinkerton F E, Meyer M S, Meisner G P, et al. Improved hydrogen release from LiB$_{0.33}$N$_{0.67}$H$_{2.67}$ with noble metal additions. J Phys Chem B, 2006, 110: 7967–7974

30 Orimo S, Nakamori Y, Kitahara G, et al. Dehydriding and rehydriding reactions of LiBH$_4$. J Alloys Compd, 2005, 404–406: 427–430

31 Pei Y, Guo P J, Qiao M H, et al. The modification effect of Fe on amorphous CoB alloy catalyst for chemoselective hydrogenation of crotonaldehyde. J Catal, 2007, 248: 303–310

32 Xu Q, Chandra M. Catalytic activities of non-noble metals for hydrogen generation from aqueous ammonia-borane at room temperature. J Power Sources, 2006, 163: 364–370

33 Liu Y F, Luo K, Zhou Y F, et al. Diffusion controlled hydrogen desorption reaction for the LiBH$_4$/2LiNH$_2$ system. J Alloys Compd, 2009, 481: 473–479